J. Membrane Biol. 185, 145–155 (2002)
DOI: 10.1007/s00232-001-0122-1

The Journal of
Membrane
Biology

Mutation D384N Alters Recovery of the Immobilized Gating Charge in Rat Brain IIA Sodium Channels

F.J.P. Kühn, N.G. Greeff
Physiologisches Institut, Universität Zürich, Winterthurerstr. 190, CH-8057 Zürich, Switzerland

Received: 22 May 2001/Revised: 29 September 2001

Abstract. Rat brain (rBIIA) sodium channel fast inactivation kinetics and the time course of recovery of the immobilized gating charge were compared for wild type (WT) and the pore mutant D384N heterologously expressed in *Xenopus* oocytes with or without the accessory β_1-subunit. In the absence of the β_1-subunit, WT and D384N showed characteristic bimodal inactivation kinetics, but with the fast gating mode significantly more pronounced in D384N. Both, for WT and D384N, coexpression of the β_1-subunit further shifted the time course of inactivation to the fast gating mode. However, the recovery of the immobilized gating charge (Q_g) of D384N was clearly faster than in WT, irrespective of the presence of the β_1-subunit. This was also reflected by the kinetics of the slow I_g OFF tail. On the other hand, the voltage dependence of the Q_g-recovery was not changed by the mutation. These data suggest a direct interaction between the selectivity filter and the immobilized voltage sensor S4D4 of rBIIA sodium channels.

Key words: Sodium channel — Bimodal gating — Pore mutation — Immobilization — Voltage sensor

Introduction

Voltage-dependent ion channels display two main functions, the gating mechanism, i.e., the opening and closing of the pore, and the conduction mechanism, i.e., the selection and translocation of the permeating ions. Initially, these two processes were regarded to be structurally and functionally independent (Hodgkin & Huxley, 1952). In fact, several mutations have been described that affect either activation or inactivation gating without significantly changing the permeation properties of the channels (Chahine et al., 1994; McPhee et al., 1998).

However, recent studies suggest a functional coupling between gating and permeation (Tomaselli et al., 1995; Balser et al., 1996; Wang & Wang, 1997; Townsend & Horn, 1999; Bénitah et al., 1999; Vilin et al., 1999). For instance, Tomaselli et al. (1995) have demonstrated that the single point mutation W402C in the P-loop of domain 1 of the μ1 sodium channel has a strong impact on channel gating including acceleration of activation, whole-cell current decay and recovery from inactivation.

Hitherto, a series of experimental data supports the hypothesis that in voltage-gated sodium channels the S4 voltage sensor of domain 4 (S4D4) is particularly involved in the process of fast inactivation (Chahine et al., 1994, Yang, George & Horn, 1996; Chen et al., 1996; Kontis & Goldin, 1997; McPhee et al., 1998; Kühn & Greeff, 1999; Sheets et al., 1999).

On the other hand, the β_1-subunit that presumably interacts with the P-loops of domain 1 and 4 (Makita, Bennett & George, 1996; McCormick et al., 1998), in some cases, reduces the bimodal gating behavior of the sodium channel α-subunit, if expressed in *Xenopus* oocytes (Isom et al., 1992; Cannon, MacClatchey & Gusella, 1993; Bennett, Makita & George, 1993; Patton et al., 1994). Moreover, binding studies of both, site-3 toxins and the β_1-subunit, suggest that domains 1 and 4 must be closely adjacent in the sodium channel tertiary structure (Rogers et al., 1996; Makita et al., 1996). The movement of S4D4 and thus especially the inactivation gating were strongly influenced by site-3 toxins (Hanck & Sheets, 1995; Sheets et al., 1999), most probably by an electrostatic mechanism. Presumably, other extracellular determinants of gating modulation, like the β_1-subunit, μ-Conotoxins or fixed surface charges, work in a similar manner (French et al., 1996; Bennett et al., 1997; McCormick et al., 1998; Elinder & Århem, 1999).

Correspondence to: F.J.P. Kühn. email: fkuehn@physiology.rwth-aachen.de

The outer pore structure of the rBIIA sodium channel contains several residues that contribute to the binding of the guanidinium toxins Tetrodotoxin and Saxitoxin (TTX and STX; Noda et al., 1989; Terlau et al., 1991; Satin et al., 1992; Penzotti et al., 1998). Furthermore, it was shown that the guanidinium toxin binding site is located partially within the transmembrane electric field (Satin et al., 1994). The mutation D384N, located in the P-loop of domain 1 of the rBIIA sodium channel, drastically reduces both, the guanidinium toxin sensitivity and the pore permeability, without preventing its gating function (Pusch et al., 1991). Although it was possible to record the readily detectable gating current (*I*g) of D384N, the extremely low single-channel conductance of this mutant, estimated by Pusch et al. (1991) to be about three orders of magnitude lower than for WT, until now has prevented the characterization of the corresponding ionic current (I_{Na}) kinetics.

In our study we succeeded in the recording of both I_{Na} and I_g of WT and mutant rBIIA sodium channels using a high expression system in *Xenopus* oocytes and an optimized two-electrode voltage clamp (Kühn & Greeff, 1999; Greeff & Kühn, 2000). Therefore, we were able to compare the gating kinetics of WT and D384N in more detail in order to analyze the interaction between the outer pore region and voltage-sensor movement during recovery from fast inactivation.

Materials and Methods

Mutagenesis and Expression of Channels

The cDNAs of both, the wild-type rat brain IIA (rBIIA) sodium channel α-subunit (according to the new nomenclature identical to rNa_v 1.2a) and the rat brain β_1-subunit used in this study, were derived from plasmid pVA2580 and pBluescript SK-, respectively, and transferred into the high-expression vector pBSTA as described elsewhere (Patton et al., 1994; Greeff & Kühn, 2000). The resulting plasmids pBSTA(α) and pBSTA(β) contain a T7 RNA polymerase promotor and *Xenopus*-β-globin 5′and 3′ untranslated sequences that greatly increase the expression of exogenous proteins in oocytes (Shih et al., 1998). Site-directed mutagenesis was performed using the QuikChange mutagenesis system (Stratagene, La Jolla, CA). Mutagenic oligonucleotides were designed such that restriction endonuclease recognition sites were created or deleted. Therefore, the desired mutations could be quickly identified by restriction analysis of the recombinant plasmid clones. In addition, every mutation was verified by DNA sequencing. Two independent clones of each mutant were tested to exclude effects of inadvertent mutations in other regions of the channel. Capped, full- length transcripts were generated from *SacII* linearized plasmid DNA using T7 RNA polymerase (mMessage mMachine In Vitro Transcription Kit from Ambion, Austin, TX). Large oocytes (stage V–VI; 1.2 mm diameter on average) from *Xenopus laevis* (NASCO, Ft. Atkinson, WI) were used. For surgical removal of the oocytes, female frogs were anesthetized with 0.15% tricaine (3-aminobenzoic acid ethyl ester; Sigma, St. Louis, MO) and placed on ice. Frogs were allowed to recover at least 6 months following surgery. All animal handling was carried out in accordance with methods approved by Swiss Government authorities.

One day before injection of complementary RNA (cRNA), the oocytes were defolliculated in a Ca^{2+}-free solution containing 2 mg/ml collagenase (Boehringer, Mannheim, Germany), for ~2 hr at room temperature. Oocytes were microinjected with 50–100 ng of cRNA (50 nl) and maintained at 18 ± 1°C in Modified Barth's Solution (MBS, in mM): 88 NaCl, 2.4 $NaHCO_3$ 1 KC1, 0.82 $MgSO_4$, 0.41 $CaCl_2$, 0.33 $Ca(NO_3)_2$, 10 HEPES-CsOH, pH 7.5, supplemented with 25 U penicillin, 25 μg/ml streptomycin-sulfate and 50 μg/ml gentamycin-sulfate. For the recording of uncontaminated I_g, TTX (RBI-Research Biochemicals International, Natick, MA) or STX (Calbiochem, La Jolla, CA) was added.

Electrophysiology and Data Acquisition

Two-electrode voltage-clamp recordings were performed 3 to 8 days after cRNA-injection with a TEC-05 (npi-electronic, Tamm, Germany) that had been modified for improved compensation of the series resistance (R_s) and for fast charging of the membrane capacitance (Greeff & Polder, 1998; Greeff & Kühn, 2000). Intracellular agarose cushion electrodes (Schreibmayer, Lester & Dascal, 1994) were filled with 3 M KCl and had a resistance between 50 and 100 kΩ. Macroscopic I_{Na} and I_g signals were recorded using a PDP-11/73 computer (Digital Equipment, Maynard, MA) controlling a 16-bit A/D and 12-bit D/A interface (CED, Cambridge, UK). The oocytes were clamped at a holding potential of −100 mV for at least 5 minutes to ensure recovery from slow inactivation before recording started. The experiments were done at a temperature of +15 ± 1°C, controlled by a Peltier element, unless otherwise stated. R_s-compensation was adjusted to accelerate the settling time of the capacitance transients within 200 μsec. No analog subtraction was used, since the 16-bit ADC had a sufficiently fine resolution for digital subtraction of the linear transient and leak currents by scaled averages from pulses between −120 mV and −150 mV. Data analysis was performed on the PDP-11 and additionally with the Windows-compatible programs UN-SCAN-IT™ (Silk Scientific, Orem, UT) and PRISM™ (GraphPad Software, San Diego, CA).

Results

Expression and Sensitivity to TTX and STX

Figure 1 illustrates typical recordings of I_{Na} and I_g obtained from the whole-cell membrane of *Xenopus* oocytes injected with either wild-type (WT) or mutant (D384N) cRNA and recorded in the presence or in the absence of the guanidinium toxins TTX or STX in the bath solution. We found that I_{Na} of WT channels usually is blocked by 2 μM TTX, whereas I_{Na} of D384N channels is effectively suppressed only by 15 μM STX (Fig. 1). Interestingly, the slow OFF-gating current (I_gOFF) tail observed in D384N displayed a time course that was quite different from WT, as already noted by Pusch et al. (1991). This characteristic I_gOFF was prominent even in the presence of 15 μM STX (See Fig. 1), indicating that it was not caused by I_{Na}.

The expression of rBIIA sodium channels in our study was very effective and I_{Na} recordings of up to

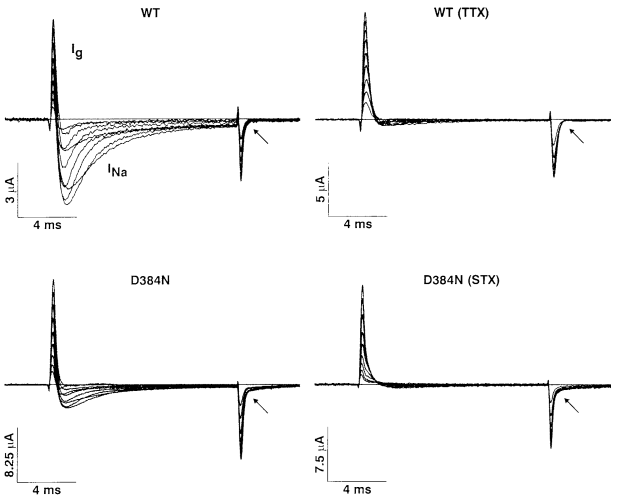

Fig. 1. High expression of I_{Na} and I_g of WT and D384N sodium channels—sensitivity to guanidinium toxins. Recordings were performed after 4 to 6 days of incubation and currents were elicited by step depolarizations from −40 mV to 40 mV in increments of 10 mV. Test pulse duration was 13 msec, holding potential −100 mV. The application of 2 μM TTX for WT or 15 μM STX for D384N during recording abolished almost all I_{Na} as visible. In order to display both I_g and I_{Na} well resolved in the same recording for WT, I_{Na} was partially blocked by TTX. Note the different kinetics of the slow I_gOFF tail of WT and D384N even in the absence of I_{Na} (indicated by arrows).

150 μA for WT and 3 μA for D384N, as well as I_g recordings of up to 10 and 15 μA for WT and D384N, respectively, could be achieved. Series resistance (R_s) errors were < 5 mV unless the currents exceeded 30–40 μA, because an improved two-electrode voltage clamp was used (see Greeff & Kühn, 2000). Note that the shown WT I_{Na} were obtained in partial and full TTX blockade to have them comparable in size to the mutant I_{Na} and to minimize R_s errors. The I/V dependence appears normal in that the largest inward current occurs at −10 mV. The small and slow traces at −30 and −40 mV have unusually early peaks, which may originate from membrane regions at the bottom of the cell, which are not homogenously blocked by TTX.

Time Course of Fast Inactivation

The use of a high-expression system together with the recording of currents in the whole-cell configuration for the first time made it possible to compare the I_{Na} kinetics of D384N and WT. Representative current traces of WT with and without β_1-coexpression, as well as of D384N elicited by depolarizing pulses to −20 mV, 0 mV and 20 mV from a holding potential of −100 mV and recorded after 6 days of incubation, are shown in Fig. 2. The data were well fit to a double-exponential curve yielding inactivation time constants as indicated in the legend of Fig. 2. In the absence of the β_1-subunit, the I_{Na} of WT displayed a pronounced biphasic decay reflecting the presence of a mixture of a fast and a prominent proportion of slow gating channels with corresponding inactivation time constants determined, e.g., at 0 mV of 1.2 msec and 11.7 msec, respectively (Fig. 2*A*). This phenomenon is typical for the expression of brain and skeletal-muscle sodium channel α-subunits in *Xenopus* oocytes (e.g., Patton et al., 1994). Correspondingly, in the presence of β_1, the fast gating mode was strongly favored (Fig. 2*B*) and in addition the inactivation time constants of both kinetic populations were decreased. For example, at 0 mV the inactivation time constants of WT-($\alpha+\beta_1$) were 0.7 msec (fast mode) and 7.0 msec (slow mode). As derived from Fig. 2*C*, also D384N-α showed bimodal gating behavior, but with the fast gating mode significantly more pronounced than in WT-α (Fig. 2*A*), even if not as prominent as observed for coexpression of WT-α with β_1 (Fig. 2*B*). Actually, Fig. 3*B* shows that the macroscopic I_{Na} decay of D384N-α was further shifted to the fast gating mode by coexpression of the β_1-subunit. The corresponding inactivation time constants of D384N-α, determined at depolarizing voltages of 0 mV, were 0.8 msec, (fast mode) and 8.5 msec (slow mode) and, therefore, similar to WT-($\alpha+\beta_1$).

It should be noted at this point that the impact of the β_1-subunit on the inactivation kinetics of D384N could not be studied in more detail because the ratio between the recorded I_{Na} and the inevitably associated large I_g of D384N + β_1 was consistently too small and, therefore, the corresponding time course of I_{Na} was markedly distorted by I_g (*see* Fig. 3*B*). We tried to obtain pure I_{Na} traces by digital subtraction of subsequent recordings of step depolarizations in the presence or absence of 15 μM STX. However, the resulting data were not convincing (*not shown*).

I_{Na}-Recovery from Fast Inactivation in the Presence or in the Absence of the β_1-Subunit

The similar bimodal gating behavior of WT and D384N sodium channels became also evident considering the I_{Na} recovery from fast inactivation (Fig. 3). The superimposed current traces elicited for recovery intervals increasing logarithmically from 1 msec to 256 msec demonstrate that for WT-α and D384N-α only the fast-mode channels finished recovery within 256 msec. The recovery of the slow-mode channels remained incomplete (Fig. 3*A* and *B*). This was especially observed for WT-α where, as already demonstrated in the data of Fig. 2, the slow gating mode was significantly more pronounced. In contrast, the recovery of WT-($\alpha+\beta_1$) and D384N-($\alpha+\beta_1$) was almost complete within 256 msec, reflecting the principal shift to the fast gating mode induced by the β_1-subunit both, in WT and D384N.

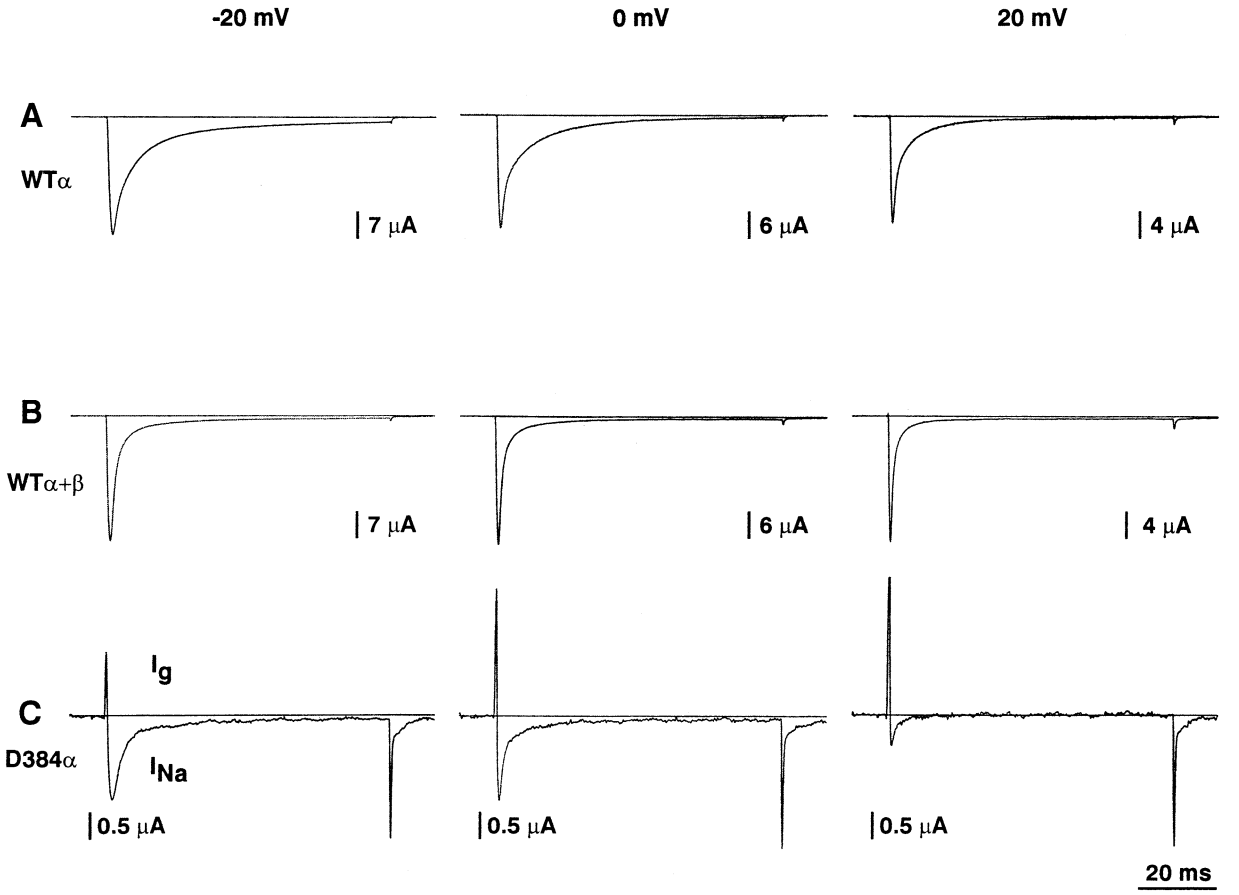

Fig. 2. Effects of pore mutation D384N and β_1-coexpression on the I_{Na}-inactivation kinetics. (*A–C*) Comparison of typical single current traces of WT in the absence (*A*) or in the presence (*B*) of the β_1-subunit and of mutant D384N (*C*) elicited after 6 days of incubation by depolarizing pulses to −20, 0 and 20 mV, as indicated; holding potential −100 mV; test pulse duration 80 msec. The data were fitted to a double-exponential curve according to the equation: $Y = A1 \cdot \exp(-X/T1) + A2 \cdot \exp(-X/T2) + L$ with inactivation time constants ($\tau_{h\ (fast)}/\tau_{h\ (slow)}$ in msec) WT-α: 2.3/12.5 (−20 mV), 1.2/11.7 (0 mV), 0.8/7.6 (20 mV); WT-(α+β): 1.0/8.5 (−20 mV), 0.7/7.0 (0 mV), 0.5/4.2 (20 mV) and D384N-α: 1.8/17.5 (−20 mV), 0.8/8.5 (0 mV), 0.6/3.9 (20 mV).

To check for current decay during pulse series, we used an alternating pulse protocol for each recovery time interval with a test pulse in the absence of a prepulse (indicated as *F1* in Fig. 3), immediately followed by a test pulse in the presence of an inactivating prepulse (indicated as *F2* in Fig. 3). Because we used inactivating prepulses of only 100 msec duration and the time interval between subsequent *F1* test pulses was about 2 sec, slow inactivation effects seemed rather unlikely. Therefore, the current decay of *F1* observed especially in WT-α and less in D384N-α (Fig. 3*A* and *B*) most probably was due to the slower recovery of the slow-mode channels. In contrast, with the β_1-subunit coexpressed, both, WT and D384N, displayed no significant current decay in *F1* (Fig. 3*A* and *B*), which reflects a smaller proportion of channels that gate in the slow mode.

These results demonstrate that the fast inactivation kinetics of D384N-α were significantly accelerated, if compared to WT-α. However, the corresponding modulating effects of the β_1-subunit (shift to the fast gating mode and decrease of the time constants) clearly exceeds the impact of the pore mutation.

Kinetics of the Slow I_gOFF Tail Current and Recovery from Voltage-Sensor Immobilization

One of the most striking differences between WT and D384N was the kinetics of the slow I_gOFF tail (*see* Fig. 1). This was already noted by Pusch et al. (1991) and tentatively interpreted as a reflection of a faster recovery from inactivation.

Therefore, we determined the kinetics of the slow I_gOFF tails of WT and D384N (Fig. 4*B*) and compared it to the time course of the recovery from voltage-sensor immobilization (Figs. 4*C* and 5). The corresponding ON- and OFF-I_g, elicited by a step depolarization to 40 mV of 80 msec duration from a holding potential of −100 mV, are represented in Fig. 4*A*. The test pulse to approximately sodium reversal potential (E_{Na}) resulted in a nearly complete

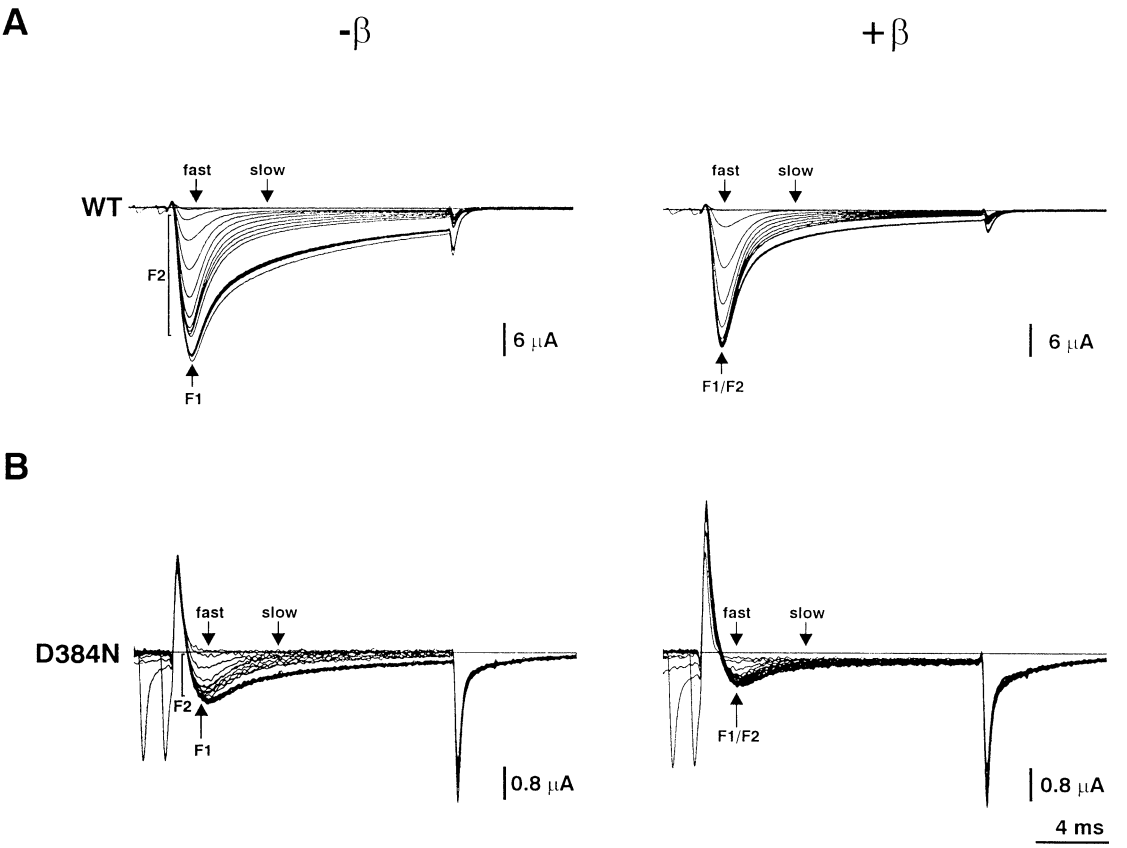

Fig. 3. I_{Na}-recovery from fast inactivation in the presence or in the absence of the β_1-subunit. Typical recordings of I_{Na} during recovery from fast inactivation of WT (*A*) and D384N (*B*) with and without coexpression of the β_1-subunit (as indicated) obtained after 4 days of incubation. The inactivating conditioning pulse to 0 mV had a duration of 100 msec; holding potential −100 mV. Inter-pulse intervals were increased logarithmically from 1 msec to 256 msec at a recovery potential of −100 mV and were followed by a 13-msec test pulse to 0 mV. Responses are superimposed for all recovery periods. Note the predominance of the fast or the slow gating mode at different points in the course of the current decay (indicated by arrows). The current traces obtained without prepulse are indicated as *F1*, whereas *F2* shows current traces generated in the presence of an inactivating conditioning pulse.

inactivation of D384N channels after 80 msec (*see* Fig. 2*C*). On the other hand, the presence of 2 μM TTX suppressed most of the I_{Na} in WT (*see* Fig. 1). Accordingly, the I_g traces were hardly distorted by I_{Na} and the determination of the corresponding time integrals Q_{ON} and Q_{OFF} for 20 msec yielded a reasonably good agreement of both values (Fig. 4*A*). The slight difference between Q_{ON} and Q_{OFF} observed in WT was due to the fact that, because of the very slow time course of recovery at −100 mV, only 80% of I_gOFF was included in the time window used. However, with faster kinetics obtained at a recovery potential of −120 mV, Q_{OFF} equals Q_{ON} already after 20 msec, (Fig. 5*C*). Nevertheless, the kinetics of the slow I_gOFF tails (Fig. 4*B*) as well as the corresponding Q_g recoveries (Figs. 4*C* and 5*A*/*B*) were obtained at a recovery potential of −100 mV, and the data were fitted to a double-exponential curve with resulting time constants included in the Figures. Generally, Q_g- recovery was determined with inactivating prepulses to 20–40 mV and test pulses to 40 mV (~E_{Na}). Figure 4*C* displays a comparison of original recordings of Q_g recovery of WT with β_1- and D384N without β_1-coexpression generated in the presence (*F2*) or in the absence (*F1*) of an inactivating conditioning pulse respectively.

First of all, Fig. 4*B* shows that the time course of I_gOFF decay is significantly accelerated in D384N if compared to WT, and the resulting time constants (as indicated in the figure) agree quite well with the corresponding data obtained from Q_g recovery (Figs. 4*C* and 5). Thus, the recovery from immobilization of D384N-α was considerably faster than observed in WT-α even with β_1-coexpression, as can be derived from the comparison of the sequences of increasing I_g traces as well as from the different levels of the non-immobilized I_g at the onset of recovery (Fig. 4*C*; *see* also Fig. 6*A*). This was confirmed by the comparative analysis of the Q_g recovery kinetics of WT and D384N with and without β_1-coexpression and with data fitted to a single- or a double-exponential curve (Fig. 5, including corresponding time constants). The β_1-subunit slightly speeds up the Q_g recovery of both, WT and D384NA (Fig. 5*B*), but the impact of the

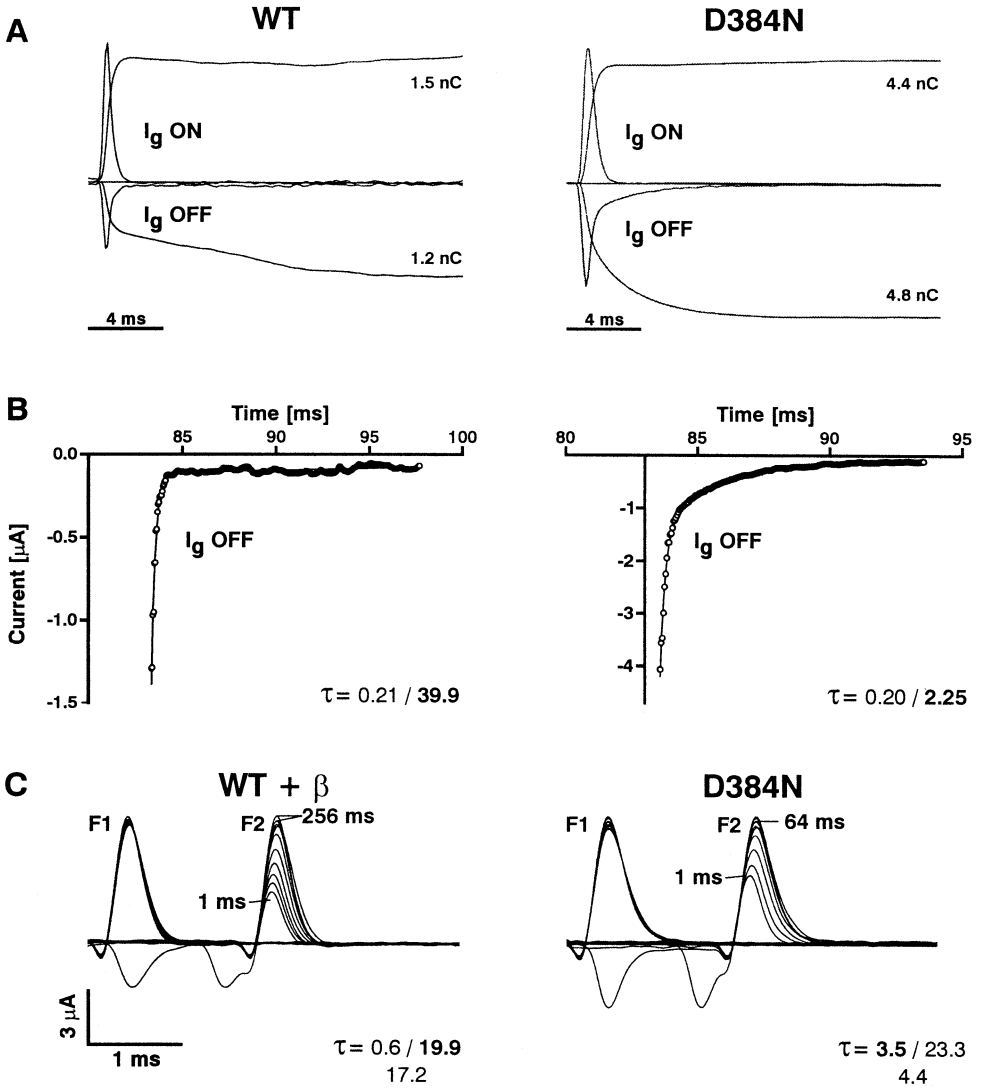

Fig. 4. Kinetics of the slow I_gOFF tail current and Q_g-recovery of WT and D384N. (*A*) Superimposed traces of corresponding ON- and OFF-I_g obtained from WT and D384N elicited by an 80-msec test pulse to 40 mV ($\approx E_{Na}$) with time integrals included for a duration of 20 msec; holding potential −100 mV. The I_g-recordings of WT were performed in the presence of 2 μM TTX. (*B*) I_gOFF-decays of *A* fitted to a double-exponential curve according to the equation: $Y = A1 \cdot \exp(-X/T1) + A2 \cdot \exp(-X/T2) + L$ with corresponding time constants as indicated (dominant time constant bold). (*C*) Original recordings of I_g during recovery from immobilization obtained from WT in the presence of the β_1-subunit and from D384N without β_1-coexpression. Same pulse protocol as described in Fig. *3A* but with test pulses to 40 mV ($\approx E_{Na}$). The superimposed traces were generated in the presence (*F2*), or in the absence (*F1*) of an inactivating conditioning pulse, respectively. For the determination of the recovery time course, *F2* was routinely normalized to *F1* and the data were fitted as described in Fig. *5A/B* with corresponding time constants in msec as indicated (dominant time constant of double-fit bold and single-fit value in second line). Note the different onsets after 1 msec of recovery and also the time needed to reach the plateau of recovery (as indicated), reflecting distinct kinetics.

pore mutation alone on the time course of recovery from voltage sensor immobilization was clearly more pronounced (Fig. *5A*).

A comparison of the Q_g recovery of WT-α and D384N-α determined at recovery potentials of −80 mV, −100 mV and −120 mV with data fitted to a single-exponential curve, is illustrated in Fig. 5*C* (resulting time constants included in the figure). For all recovery potentials tested, the time constants of D384N-α were considerably decreased if compared to WT-α, but the voltage dependence of recovery was not significantly changed.

Immobilization

In sodium channels the inactivation process is closely coupled to the partial immobilization of the gating charge (Bezanilla & Armstrong, 1975) because the inactivation lid, besides closing the open pore, also interferes with the movement of the voltage sensors of

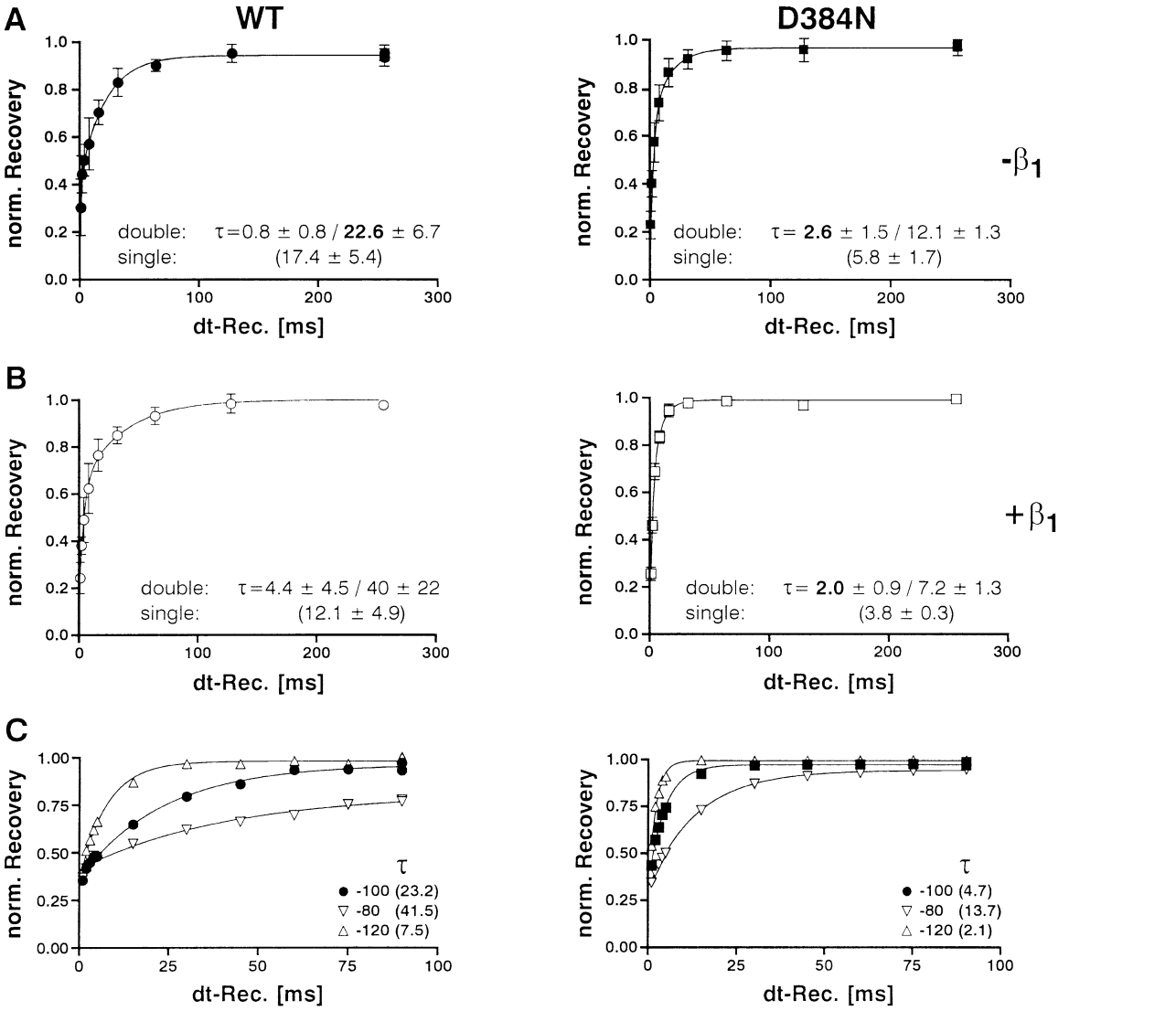

Fig. 5. Q_g-recovery in the presence or in the absence of β_1-coexpression. (*A–B*) Q_g-recovery of WT and D384N in the absence (*A*) or in the presence (*B*) of the β_1-subunit. Same pulse protocol as described in Fig. *3A* but with test pulses to 40 mV ($\approx E_{Na}$). Each data set was obtained from three separate experiments and fitted both, to a single-exponential curve according to the equation: $Y = A \cdot (1-\exp(-X/T)) + P$ (fit not shown but corresponding mean ± SEM in msec given in brackets) and to a double-exponential curve of the form: $Y = A1 \cdot (1-\exp(-X/T1)) + A2 \cdot (1-\exp(-X/T2)) + P$ with time constants (mean ± SEM in msec) as indicated (dominant time constant bold). (*C*) Typical Q_g-recoveries of WT-α and D384N-α obtained at three different recovery potentials in the course of single-cell experiments. Pulse protocol: a 50-msec prepulse to 40 mV from a holding potential of −100 mV was followed by a recovery period of variable duration (2–90 msec) at −100 mV. Test pulse was to 40 mV. The data were fitted to a single-exponential curve as described above with time constants in msec as indicated.

domains 3 and 4 (Cha et al., 1999; Sheets, Kyle & Hanck, 2000). This is also reflected by the fact that the recovery time courses of fast inactivation and of gating-charge immobilization display the same kinetics (Armstrong & Bezanilla, 1977; Kühn & Greeff, 1999). Already Pusch et al. (1991) noted that the immobilization properties of D384N differ significantly from WT and may reflect a faster recovery from inactivation.

Gating-charge immobilization in WT and D384N was determined using a two-pulse protocol (*see* Fig. 6*A*). The test pulse was preceded by a depolarizing conditioning pulse that provoked channel activation and subsequently, both channel inactivation and voltage sensor immobilization. During a brief recovery period of 1 msec duration at −100 mV, the rapid transitions between different inactivated states produced the non-immobilized fraction of the total Q_g showing fast kinetics. Simultaneously, the immobilized fraction of Q_g started to recover with a markedly slower time course, which, however, was only seen well in D384N (indicated by a dotted line in Fig. 6*B*).

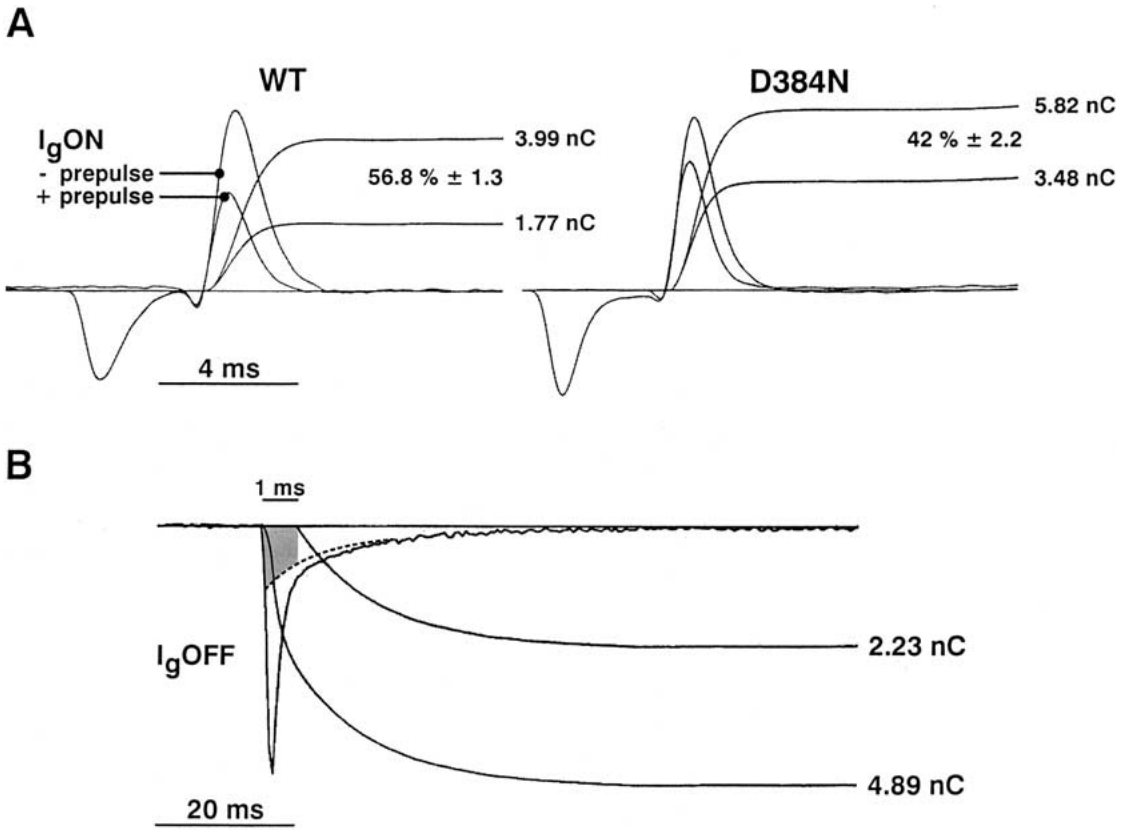

Fig. 6. Immobilization properties of WT and D384N. (*A*) Alternating pulse protocol: a 13-msec test pulse to 40 mV ($\approx E_{Na}$) was either preceded by a 20-msec conditioning pulse to 0 mV followed by a l-msec inter-pulse interval at −100 mV or not (as indicated). The traces of total gating current ($I_{g,t}$) obtained without prepulse and the fraction of non-immobilized gating current ($I_{g,n}$) plus already recovered gating current (*see B*) obtained with prepulse are superimposed in each subdiagram with corresponding time integrals (Q_g) included. The apparent degree of immobilization is indicated (mean ± SEM of $n = 5$ cells) and represents the difference between the corresponding time integrals of $I_{g,t}$ and $I_{g,n} + x$ (x = fraction of recovered Q_g after 1 msec). (*B*) Correlation of the time course of Q_g-recovery and the apparent degree of Q_g-immobilization. I_gOFF from mutant D384N recovering at −100 mV after a depolarizing pulse to 40 mV ($\approx E_{Na}$) of 80 msec duration. Two kinetic components can be clearly identified; the fast one corresponds to gating transitions between inactivated states producing the non-immobilized I_g-fraction; the slow one (illustrated by the dotted line) reflects voltage sensor recovery from immobilization. As indicated by the shaded area, during the first millisecond not only fast transitions occur but also a substantial part of immobilized channels has started to recover. Consequently, the degree of immobilization determined for D384N as described in *A* was apparently reduced if compared to WT because the Q_g-recovery of the mutant was accelerated.

In this study, the degree of immobilization was taken as the difference (100−X%) between the Q_g obtained without inactivating prepulse (100%) and the corresponding Q_g obtained in the presence of an inactivating prepulse after 1 msec of recovery at −100 mV (X%). Compared to WT (56.8%), the degree of immobilization (Fig. 6*A*) was significantly reduced in D384N (42%). The changed immobilization properties of D384N suggest that the movement of the voltage sensors 3 and/or 4 (*see* Cha et al., 1999; Kühn & Greeff, 1999) was affected by the mutation. However, the detailed analysis of D384N showed that during 1 msec at −100 mV a substantial fraction of immobilized Q_g had already recovered (shaded area in Fig. 6*B*), and, therefore, contaminated the fraction of non-immobilized Q_g in the I_gON of D384N (Fig. 6*A*). Accordingly, the degree of immobilization, as determined in this study, was only apparently reduced in D384N, because the corresponding Q_g recovery was clearly faster than in WT.

Discussion

In this study, we analyzed the inactivation kinetics of the mutation D384N located in the selectivity filter of rat brain IIA sodium channels (Terlau et al., 1991). For the first time, we succeeded in the recording of well resolved ionic currents of this mutant, even though the pore permeability was dramatically decreased (Pusch et al., 1991). Furthermore, we compared the recovery kinetics of the immobilized gating charge of WT and D384N with and without coexpression of the accessory β_1-subunit. In the light of recent data, exclusively achieved by ionic current analysis, which indicate a functional coupling

between the pore and inactivation gating (Tomaselli et al., 1995; Balser et al., 1996; Townsend & Horn, 1999; Vilin et al., 1999), we wanted to know if there is a direct impact of mutation D384N on voltage-sensor movement in the course of fast inactivation. Hitherto, only the Q/V-properties of WT and mutant D384N were compared. As a result, it was concluded that the gating processes of WT and D384N are quite similar (Pusch et al., 1991).

First of all, our analysis of the relatively small but sufficiently resolved I_{Na} in D384N demonstrated that, similar to WT, the inactivation kinetics are characterized by a mixture of fast and slow gating channels that is typical for the expression of brain (Moorman et al., 1990; Krafte et al., 1990) and skeletal muscle (Zhou et al., 1991; Bennett et al., 1993) sodium channels in *Xenopus* oocytes. However, the inactivation time course of mutant D384N was significantly more characterized by the fast gating mode and the time constants of both gating modes were decreased, if compared to WT. As previously described by Isom et al. (1992) and Patton et al. (1994), and confirmed in this study under high-expression conditions, the presence of the β_1-subunit strongly favors the fast gating mode of WT rBIIA sodium channels and in addition accelerates the kinetics of both gating modes. The impact of the β_1-subunit on the inactivation kinetics of WT-α was clearly stronger than the corresponding effect induced by the pore mutation. Moreover, the β_1-subunit further accelerated the inactivation kinetics of D384NA, suggesting that the pore mutation and β_1-coexpression induce synergistic and additive effects. This observation is supported by the findings of Makita et al. (1996) and McCormick et al. (1998) who showed that the β_1-subunit probably interacts with the P-loops of domains 1 and 4, and therefore in the vicinity of mutation D384N.

The bimodal gating behavior of WT and D384N rBIIA was also evident with respect to the time course of recovery from fast inactivation. Both, WT and D384N recovered with two different kinetics, but in D384N and even more in the presence of the β_1-subunit, the recovery time course was accelerated and shifted to the fast gating mode. Nevertheless, in D384N as well as in the presence of the β_1-subunit, the slow gating channels were not completely absent. For the β_1-subunit this was also described by others (Cannon et al., 1993; Wallner et al., 1993; Patton et al., 1994; Chang, Satin & Fozzard, 1996). Because the size of the ionic currents of D384N and WT was very different as was also the relative proportion of the corresponding I_{Na} and I_g, we faced the problem that R_s errors would possibly distort our comparative kinetic analyses. On the other hand, the high expression was necessary to record well resolved gating currents and also to detect the drastically reduced ionic current of D384N. In former studies we noted that at high expression levels the analysis of the I_g was more reliable for the characterization of the recovery kinetics of WT channels than the corresponding I_{Na} (Kühn & Greeff, 1999; Greeff & Kühn, 2000).

It has to be mentioned at this point, that it was not the aim of this study to reveal the molecular basis of the impact of the β_1-subunit on sodium channel fast inactivation kinetics. Instead, our aim was to use the β_1-coexpression as control experiment in order to show that the point mutation D384N exerts similar but less pronounced effects on the fast inactivation kinetics, when compared to the β_1-subunit, especially with respect to the gating mode shift. On the other hand, the corresponding effects on the recovery kinetics of the immobilized voltage sensor S4D4 were clearly more prominent in D384N than in β_1-coexpression (as discussed below).

During recovery not only the kinetics of unblocking the pore by the inactivation lid (measurable at the I_{Na} level) but also the kinetics of the return of the blocked voltage sensors (measurable at the I_g level) could be analyzed, and it had been clearly demonstrated that both recoveries follow the same time course (Armstrong & Bezanilla, 1977; Kühn & Greeff, 1999; Greeff & Kühn, 2000). Therefore, the impact of the mutation D384N as well as of the coexpression of the β_1-subunit on the recovery kinetics from fast inactivation was studied at the I_g level. The detailed analysis demonstrates that the faster time course of the slow I_gOFF tail current already noted by Pusch et al. (1991) actually reflects an accelerated recovery kinetics from fast inactivation, when compared to WT. The Q_g-recovery of D384N was significantly faster than in WT with or without β_1 coexpression. Consequently, the effect of the mutation D384N on the recovery time course of the immobilized Q_g was clearly stronger than achieved by coexpression of the β_1-subunit. On the other hand, the voltage dependence of Q_g recovery was not changed in D384N, which is not surprising, as the amount of the displaced charges during voltage sensor movement is not altered by the mutation.

Cha et al. (1999) have demonstrated that in sodium channels only the voltage sensors of domains 3 and 4 were immobilized during fast inactivation. On the other hand, it was shown that during repolarization the rate-limiting movement of S4D4 was independent from the binding of the inactivation lid, whereas immobilization of S4D3 depends on the manifestation of the inactivated state (Sheets et al., 2000). One major point of the conclusions of Sheets et al. (2000) is their observation that site-3 toxins, like *Anthopleura* Toxin-A or sea anemone toxin (ATX II), selectively inhibit the movement of voltage sensor S4D4, (Sheets et al., 1999). As established by us in a previous study (Kühn & Greeff, 1999), the mutation R1635H, located in the central part of voltage sensor

S4D4, drastically increases the time constants of both, recovery from fast inactivation and recovery from voltage-sensor immobilization and, therefore, exerts one of the strongest effects on the fast inactivation kinetics of all voltage-sensor mutants previously described (Chahine et al., 1994; Chen et al., 1996; Kontis & Goldin, 1997). However, in the presence of 2 μM ATX II we found that the recovery kinetics of WT and R1635H are indistinguishable and very fast (unpublished results), supporting the conclusions of Sheets et al. (2000) that the movement of voltage sensor S4D4 is actually inhibited by the toxin and is the rate-limiting step during recovery from immobilization.

The impact of site-3 toxins on the movement of S4D4 could be well explained by an electrostatic mechanism where the positively charged toxin interacts with the likewise positively charged outermost arginines of the voltage sensor. Consequently, the outward movement of S4D4 would be delayed by the toxin, leading to slowed inactivation kinetics and likewise, the return of the voltage sensor would be favored, which is reflected by the accelerated recovery kinetics. Indeed, this assumption was supported by the experimental data of others (e. g. Chahine, Plante & Kallen, 1996; Benzinger, Tonkovich & Hanck, 1999) and our own results (Kathe & Greeff, 1999). Likewise, the mutation D384N might also directly change the electrostatic environment due to the neutralization of the negative charge or, in other words, by shifting the surface charge to more positive values. Thus, it is conceivable that the mutation D384N exerts similar effects on the mobility of S4D4 as observed in the presence of site-3 toxins. This hypothesis was also supported by the proposed sodium channel tertiary structure where domains 1 and 4 are closely adjacent (Rogers et al., 1996; Makita et al., 1996).

Therefore, we suggest that the mutation D384N in the selectivity filter selectively accelerates the recovery kinetics of voltage sensor S4D4, presumably by an electrostatic mechanism. However, the impact of mutation D384N on the inactivation time course of rat brain IIA sodium channels was negligible, if compared to the corresponding effect obtained by site-3 toxins. While ATX and related compounds drastically destabilize the inactivated state, inducing a pronounced plateau current (Hanck & Sheets, 1995; Benzinger et al., 1999), the pore mutation only moderately shifts the inactivation kinetics to the fast gating mode. Thus, the outward movement of S4D4 is most probably not affected by the mutation D384N. The association of an external pore residue with sodium channel inactivation gating was also demonstrated by Balser et al. (1996). Their data show that the single point mutation W402C, located in the P-loop of domain 1 of μl rat skeletal muscle sodium channel, accelerated both, whole-cell current decay and recovery from inactivation. In view of these results our data represent additional evidence for an interaction between the pore and the rate of voltage-sensitive transitions.

Vilin et al. (1999) concluded from their data that both, the β_1-subunit and the P-loops, possibly interact with the slow inactivation gate of sodium channels. Such slow inactivation was not addressed in the study reported here, and therefore, we exclusively used pulse protocols where slow inactivation effects were negligible. Instead, our data showed that the moderate current decay observed in WT-α during pulse series, as well as the incomplete recovery observed in the absence of the β_1-subunit, were due to the predominance of slow gating channels.

We thank Dr. Alan L. Goldin (Irvine, CA, USA) for providing the cDNA of the wild-type rat brain IIA sodium channel (pVA2580) and the high-expression vector (pBSTA). Furthermore, we are pleased to thank Dr. William A. Catterall (Seattle, WA) for providing the cDNA of the β_1-subunit, Reiner Polder (npi electronic GmbH, Tamm, Germany) for his support in developing the modified two-electrode voltage clamp and Christian Gasser (Zürich, Switzerland) for his graphical assistance. The work was supported by the Swiss National Science Foundation (grant No. 31-37987.93.) and the Hartmann-Müller-Stiftung.

References

Armstrong, C.M., Bezanilla, F. 1977. Inactivation of the sodium channel. II: Gating current experiments. *J. Gen. Physiol.* **70:**567–590

Balser, J.R., Nuss, H.B, Chiamvimonvat, N., Pérez-García, M.T., Marbán, E., Tomaselli, G.F. 1996. External pore residue mediates slow inactivation in μ1 rat skeletal muscle sodium channels. *J. Physiol.* **494:**431–442

Bénitah, J.-P., Chen, Z., Balser, J.R., Tomaselli, G.F., Marbán, E. 1999. Molecular dynamics of the sodium channel pore vary with gating: Interactions between P-segment motions and inactivation. *J. Neurosc.* **19:**1577–1585

Bennett, P.B., Makita, N., George, A.L. Jr. 1993. A molecular basis for gating mode transitions in human skeletal muscle sodium channels. *FEBS Lett.* **326:**21–24

Bennett, E., Urcan, M.S., Tinkle, S.S., Koszowski, A.G., Levinson, S.R. 1997. Contribution of sialic acid to the voltage dependence of sodium channel gating. *J. Gen. Physiol.* **109:**327–343

Benzinger, G.R., Tonkovich, G.S., Hanck, D.A. 1999. Augmentation of recovery from inactivation by site-3 Na channel toxins. *J. Gen. Physiol.* **113:**333–346

Bezanilla, F., Armstrong, C.M. 1975. Kinetic properties and inactivation of the gating currents of sodium channels in squid axon. *Phil. Trans. Roy. Soc. B.* (*Lond*). **270:**449–458

Cannon, S.C., MacClatchey, A.I., Gusella, J.F. 1993. Modification of Na^+ current conducted by the rat skeletal muscle α subunit by coexpression with a human brain β subunit. *Pfluegers Arch.* **423:**155–157

Cha, A., Ruben, P.C., George, A.L. Jr., Fujimoto, E., Bezanilla, F. 1999. Voltage sensors in domains III and IV, but not I and II are immobilized by Na^+ channel fast inactivation. *Neuron.* **22:**73–87

Chahine, M., George, A.L., Jr., Zhou, M., Ji, S., Sun, W., Barchi, R.L., Horn, R. 1994. Sodium channel mutations in paramyotonia congenita uncouple inactivation from activation. *Neuron.* **12:**281–294

Chahine, M., Plante, E., Kallen, R.G. 1996. Sea anemone toxin (ATX II) modulation of heart and skeletal muscle sodium channel α-subunits expressed in tsA201 cells. *J. Membrane Biol.* **152:**39–48

Chang, S.Y., Satin, J., Fozzard, H.A. 1996. Modal behavior of the μ1 Na^+ channel and effects of coexpression of the β_1-subunit. *Biophys. J.* **70:**2581–2592

Chen, L.-Q., Santarelli, V., Horn, R., Kallen, R.G. 1996. A unique role for the S4 segment of domain 4 in the inactivation of sodium channels. *J. Gen. Physiol.* **108:**549–556

Elinder, F., Århem, P. 1999. Role of individual surface charges of voltage-gated K channels. *Biophys. J.* **77:**1358–1362

French, R.J., Prusak-Sochaczewski, E., Zaponi, G.W., Becker, S., Shavantha Kularatna, A., Horn, R. 1996. Interactions between a pore-blocking peptide and the voltage sensor of the sodium channel: An electrostatic approach to channel geometry. *Neuron.* **16:**407–413

Greeff, N.G., Kühn, F.J.P. 2000. Variable ratio of permeability to gating charge of rBIIA sodium channels and sodium influx in *Xenopus* oocytes. *Biophys. J.* **79:**2434–2453

Greeff, N.G., Polder, H.R. 1998. Optimization of a two-electrode voltage clamp for recording of sodium ionic and gating currents from *Xenopus* oocytes. *Biophys. J.* **74:**A402

Hanck, D.A., Sheets, M.F. 1995. Modification of inactivation in cardiac sodium channels: ionic current studies with anthopleurin-A toxin. *J. Gen. Physiol.* **106:**601–616

Hodgkin, A.L., Huxley, A.F. 1952. A quantitative description of membrane current and its application to conduction and excitation in nerve. *J. Physiol.* **117:**500–544

Isom, L.L., De Jongh, K.S., Patton, D.E., Reber, B.F.X., Offord, J., Charbonneau, H., Walsh, K., Goldin, A.L., Catterall, W.A. 1992. Functional coexpression of the β-1 subunit of the rat brain sodium channel. *Science.* **256:**839–842

Kathe, W., Greeff, N.G. 1999. Effects of sea anemone toxin II (ATX II) on the gating current of rat brain IIA Na channels expressed in *Xenopus* oocytes. *Biophys. J.* **76:**A80

Kontis, K.J., Goldin, A. 1997. Sodium channel inactivation is altered by substitution of voltage sensor positive charges. *J. Gen. Physiol.* **110:**403–413

Krafte, D.S., Goldin, A.L., Auld, V.J., Dunn, V.J., Davidson, N., Lester, H.A. 1990. Inactivation of cloned Na channels in *Xenopus* oocytes. *J. Gen. Physiol.* **96:**689–706

Kühn, F.J.P., Greeff, N.G. 1999. Movement of voltage sensor S4 in domain 4 is tightly coupled to sodium channel fast inactivation and gating charge immobilization. *J. Gen. Physiol.* **114:**167–183

Makita, N., Bennett, P.B., George, A.L. Jr. 1996. Molecular determinants of β_1 subunit-induced gating modulation in voltage-dependent Na^+ channels. *J. Neurosc.* **16:**7117–7127

McCormick, K.A., Isom, L.L., Ragsdale, D., Smith, D., Scheuer, T., Catterall, W.A. 1998. Molecular determinants of Na^+ channel function in the extracellular domain of the β_1 subunit. *J. Biol. Chem.* **273:**3954–3962

McPhee, J.C., Ragsdale, T.S., Scheuer, T., Catterall, W.A. 1998. A critical role for the S4-S5 intracellular loop in domain IV of the sodium channel α-subunit in fast inactivation. *J. Biol. Chem.* **273:**1121–1129

Moorman, J.R., Kirsch, G.E., VanDongen, A.M.J., Joho, R.H., Brown, A.M. 1990. Fast and slow gating of sodium channels encoded by a single mRNA. 1990. *Neuron.* **4:**243–252

Noda, M., Suzuki, H., Numa, S., Stühmer, W. 1989. A single point mutation confers tetrodotoxin and saxitoxin insensitivity on the sodium channel II. *FEBS Lett.* **259:**213–216

Patton, D.E., Isom, L.L., Catterall, W.A,, Goldin, A.L. 1994. The adult rat brain β_1 subunit modifies activation and inactivation gating of multiple sodium channel α subunits. *J. Biol. Chem.* **269:**17649–17655

Penzotti, J.L., Fozzard, H.A., Lipkind, G.M., Dudley, S.C. Jr. 1998. Differences in Saxitoxin and Tetrodotoxin binding revealed by mutagenesis of the Na^+ channel outer vestibule. *Biophys. J.* **75:**2647–2657

Pusch, M., Noda, M., Stühmer, W., Noda, S., Conti, F. 1991. Single point mutation of the sodium channel drastically reduces the pore permeability without preventing its gating. *Eur. Biophys. J.* **20:**127–133

Rogers, J.C., Qu, Y., Tanada, T.N., Scheuer, T., Catterall, W.A. 1996. Molecular determinants of high affinity binding of α-Scorpion Toxin and Sea Anemone Toxin in the S3-S4 extracellular loop in domain IV of the Na^+ channel α subunit. *J. Biol. Chem.* **271:**15950–15962

Satin, J., Kyle, J., Chen, M., Bell, P., Cribbs, K,, Fozzard, H., Rogart, R. 1992. A mutant of TTX-resistant cardiac sodium channels with TTX-sensitive properties. *Science.* **256:**1202–1205

Satin, J., Limberis, J.T., Kyle, J.W., Rogart, R.B., Fozzard, H.A. 1994. The saxitoxin/tetrodotoxin binding site on the cloned rat brain IIA Na channel is in the transmembrane electric field. *Biophys. J.* **67:**1007–1014

Schreibmayer, W., Lester, H.A., Dascal, N. 1994. Voltage clamping of *Xenopus laevis* oocytes utilizing agarose-cushion electrodes. *Pfluegers Arch.* **426:**453–458

Sheets, M.F., Kyle, J.W., Kallen, R.G., Hanck, D.A. 1999. The Na channel voltage sensor associated with inactivation is localized to the external charged residues of domain IV, S4. *Biophys. J.* **77:**747–757

Sheets, M.F., Kyle, J.W., Hanck, D.A. 2000. The role of the putative inactivation lid in sodium channel gating current immobilization. *J. Gen. Physiol.* **115:**609–619

Shih, T.M., Smith, R.D,, Toro, L., Goldin, A.L. 1998. High-level expression and detection of ion channels in *Xenopus* oocytes. *Meth. Enzymol.* **293:**529–556

Terlau, H., Heinemann, S.H., Stühmer, W., Pusch, M., Conti, F., Imoto, K., Numa, S. 1991. Mapping the site of block by tetrodotoxin and saxitoxin of sodium channel II. *FEBS Lett.* **293:**93–96

Tomaselli, G.F., Chiamvimonvat, N., Nuss, H.B., Balser, J.R., Pérez-García, M.T., Xu, R.H., Orias, D.W., Backx, P.H., Marbán, E. 1995. A mutation in the pore of the sodium channel alters gating. *Biophys. J.* **68:**1814–1827

Townsend, C., Horn, R. 1999. Interaction between the pore and a fast gate of the cardiac sodium channel. *J. Gen. Phys.* **113:**321–332

Vilin, Y.Y., Makita, N., George, A.L. Jr., Ruben, P.C. 1999. Structural determinants of slow inactivation in human cardiac and skeletal muscle sodium channels. *Biophys. J.* **77:**1384–1393

Wallner, M., Weigl, L., Meera, P., Lotan, I. 1993. Modulation of the skeletal muscle sodium channel α-subunit by the β_1-subunit. *FEBS Letters.* **336:**535–539

Wang, S.-Y., Wang, G.K. 1997. A mutation in segment I-S6 alters slow inactivation of sodium channels. *Biophys. J.* **72:**1633–1640

Yang, N.B., George A.L. Jr., Horn, R. 1996. Molecular basis of charge movement in voltage-gated sodium channels. *Neuron.* **16:**113–122

Zhou, J., Potts, J.F., Trimmer, J.S., Agnew, W.S., Sigworth, F.J. 1991. Multiple gating modes and the effect of modulating factors on the μ1 sodium channel. *Neuron.* **7:**775–785